Proceedings of the 38th Chinese Control Conference
July 27-30, 2019, Guangzhou, China

Model-Assisted Extended State Observer based Repetitive Control for High Precision Tracking of Piezoelectric Nanopositioning Stages

Zhao Feng[1], Jie Ling[1], Min Ming[1], Xiaohui Xiao[1,2]
1. School of Power and Mechanical Engineering, Wuhan University, Wuhan 430072, P. R. China
E-mail: xhxiao@whu.edu.cn
2. Shenzhen Institute of Wuhan University, Shenzhen 518057, P. R. China

Abstract: High precision tracking of periodic trajectories is eagerly desired in many applications that utilize piezoelectric nanopositioning stages. Although repetitive control (RC) can improve tracking performance for commonly-used periodic reference input, it is sensitive to unexpected or non-periodic disturbances that deteriorate tracking precision. In order to achieve the anticipated performance, in this paper, a new control scheme of model-assisted extended state observer (MESO) based RC (MESORC) is developed, where MESO is utilized to estimate as well as compensate disturbances and the estimated state variables are also used to design state feedback based RC for a non-minimum phase (NMP) system with disturbances. To validate the effectiveness of the proposed method, comparative experiments are performed on a piezoelectric nanopositioning stage. Experimental results indicate that the hysteresis is suppressed effectively and the proposed method achieves the highest precision tracking of 40Hz triangular reference with delta and chirp disturbances comparing with proportional plus derivative controller and traditional RC.

Key Words: Piezoelectric Nanopositioning Stages, Repetitive Control, Extended State Observer

1 Introduction

The piezoelectric nanopositioning stage has became an important component to achieve high-precision tracking or positioning for nanometer or sub-nanometer resolution in many applications, such as atomic force microscopes (AFMs) [1], surgical device [2], ultra-precision machine tools [3] and so on for the rapid develop of nanotechnology. These stages have the advantages of the high stiffness and fast response time through employing piezoelectric actuators and flexure-hinge-guided mechanisms. [4]. However, the inherent hysteresis nonlinearities and vibrations caused by the lightly damped resonant dynamics of these stages limit the improvement of the tracking performance [5].

To handle the hysteresis nonlinearity, model-based feedforward control methods are the most common approaches via constructing inverse hysteresis models, such as Prandtl-Ishlinskii model [6], Bouc- Wen model [7] and Maxwell resistive capacitor model [8]. It should be noted that lots of parameters should be identified to improve the modeling accuracy. On the other hand, some approaches without hysteresis modeling have been proposed by treating the hysteresis as an input disturbance to simplify the controller implementation. [9–12].

However, as the the motion speed increasing, the performance is degraded severely for the lightly damped modes. Traditionally, the built-in integral or proportional-integral (PI) controllers are commonly used in commercial piezoelectric nanopositioning stages for the ease of implementation, but the closed-loop bandwidth is restricted within 2% of the first resonance frequency of the stages [1]. Therefore, many damping controllers [13] as well as modern controller, like linear quadratic Gaussian (LQG) control [14] have been proposed to impart substantial damping to improve the tracking speed and precision. Because of the fundamental algebraic restrictions in feedback, these standalone methods may not meet the required performance, such as errors caused by phase lag.

It should be noted that the periodic trajectory is commonly used in many applications, especially for the lateral motion of nanopositioning stage in AFMs [1, 5]. To cope with the issues in this motion process, it is natural to utilize repetitive control (RC) to achieve required performance as a learning type controller. The main benefit of this controller lies in that it can provide infinite gains at the fundamental frequency as well as its harmonics of the reference or disturbance based on internal model principle [15]. Compared with another learning-type controller, iterative learning control (ILC), RC does not need to reset to the initial position after each iteration, which simplifies the practical implementation [16]. However, although conventional RC can deal with periodic reference or disturbance, the error at non-periodic frequency is amplified because of waterbed effect. In [17], a dual-stage RC has been proposed to reduce the magnitude of non-periodic frequency of the sensitivity transfer function of the close-loop system via cascading conventional RC with odd-harmonic RC, which requires calculating parameters of both the RCs and the inverse hysteresis model. Besides, modified repetitive control [18] and odd-harmonic repetitive control [19] were proposed to tracking triangular signals through treating hysteresis as periodic disturbances. However, the main downside of these approaches lie in that they have not improved the ability to suppress non-periodic disturbance, which are common in piezoelectric nanopositioning stages stemmed by hysteresis, sensor noise, mechanical shocks or external environment.

In the perspective of this aspect, disturbance-observer-based control is a popular method to eliminate unexpected disturbance and model uncertainties [20]. Among these,

This work was supported by Shenzhen Science and Technology Program under Grant JCYJ20170306171514468 and China Postdoctoral Science Foundation under Grant 2018M642905.

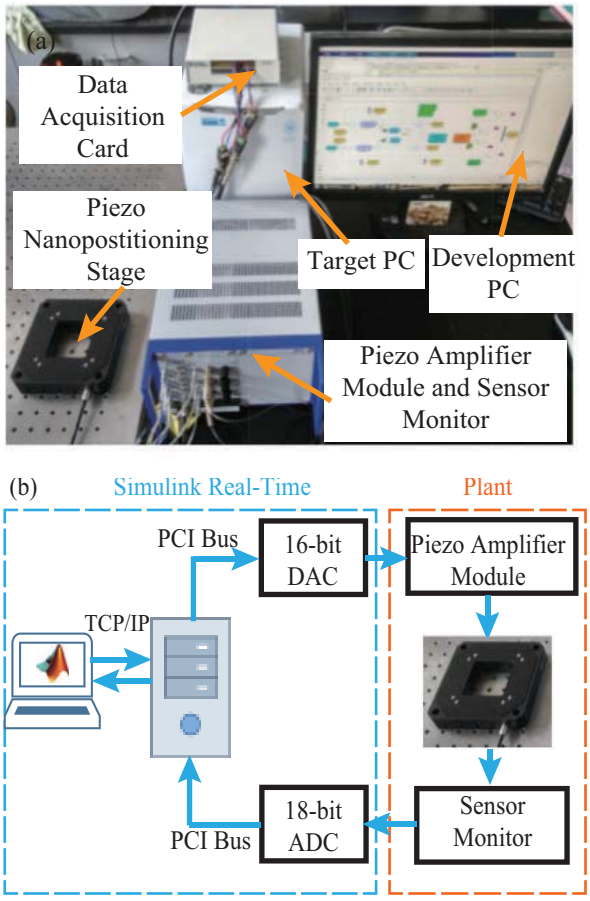

Fig. 1: The experimental setup of the piezoelectric nanopositioning stage. (a) Experimental platform. (b) Block diagram of control system.

the extended state observer (ESO) is an alternative method to estimate the disturbances by treating them as state variables. However, for non-minimum phase (NMP) systems is a challenging for traditional ESO. In [21, 22], model-assisted extended state observer (MESO) was proposed to estimate the state variables and disturbances simultaneously with the merits of a faster convergence rate and estimation accuracy.

This paper is motivated to achieve high precision motion for piezoelectric nanopositioning stages with periodic reference under disturbances. Although RC can improve reference tracking performance, it is sensitive to unexpected disturbances that do not match with the frequency of reference. In this paper, a MESO based RC is proposed, where MESO is utilized to estimate as well as compensate disturbances and the estimated state variables are also used to designed state feedback based RC for a NMP system with disturbances.

The rest of the paper is organized as follows. The system description is showed in Section 2. The controller design is presented in Section 3. Section 4 demonstrates the experiments on a piezoelectric nanopositioning stage and comparisons of the results Section 5 gives the conclusions.

2 System Description

2.1 Experimental Setup

The experimental setup is showed in Fig. 1. A piezoelectric nanopositioning stage P-561.3CD is developed to evaluate the performance. The control input voltage is generated by 16-bit digital to analog converters (DACs) via the data acquisition card PCI 6289 and subsequently amplified by a piezo amplifier module E-503.00 for the stage. The output position normalized and read via a sensor monitor E-509.C3A is passed to the data acquisition card PCI 6289 by 18-bit analog to digital converters (ADCs). The overall control system is built in Simulink Real-Time environment on the development PC, and executed real-time on the target PC. In this paper, the sample frequency of the system is set to 5 kHz.

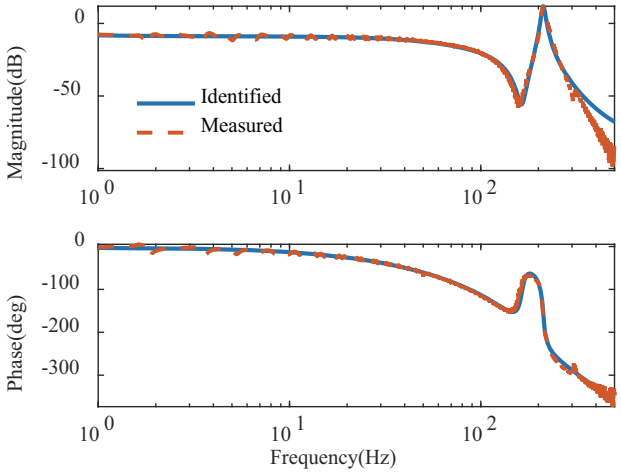

Fig. 2: Frequency response of identified and measured model with sine-sweep input.

2.2 System Identification

In order to identify the linear dynamic model of the piezoelectric nanopositioning stage without load on it, a sine-sweep input with a constant low amplitude between 0.1 Hz and 500 Hz is applied to the x axis. It should be noted that a low amplitude voltage was used to excite the system to avoid distortion from hysteresis nonlinearity. Through being discretized via zero-order holder (ZOH) method, the nominal linear discrete transfer function $P_n(z)$ with the forward time-shift operator z can be identified as

$$P_n(z) = \frac{0.012z^4 - 0.053z^3 + 0.09z^2 - 0.07z + 0.0207}{z^5 - 4.64z^4 + 8.71z^3 - 8.25z^2 + 3.95z - 0.76} \tag{1}$$

The identified and measured frequency responses are plotted in Fig.2, which indicates that Eq.1 describes the dynamics of the stage sufficiently accurately and it contains non-minimum phase zeros. It is clear that the first resonant frequency is 210 Hz from Fig.2, which limits the motion within a low speed when implementing the built-in feedback controller.

3 Controller Design

3.1 Model-Assisted Extended State Observer

Considering a single-inputsingle-output (SISO) NMP system and taking into account the disturbances, the state-space description of the above system can be written as

$$\begin{cases} x_p(k+1) = A_p x_p(k) + B_p(u(k) + d(k)) \\ y_p(k) = C_p x_p(k) \end{cases} \tag{2}$$

where $x_p(k) = [x_1(k), x_2(k), ..., x_n(k)]^{\mathrm{T}}$ is the state vector of the system and n is the order of Eq.1. $u(k)$ and $y_p(k)$ are the input and output signals of the system. A_p, B_p, C_p are the state, input, and output matrices with proper dimensions respectively. $d(k)$ is presented as an unknown combination of the system states and disturbances, such as hysteresis and external signals. Through extending the 'total disturbance' as an additional state, the augmented state space model of Eq.2 can be expressed as

$$\begin{cases} x(k+1) = A_e x(k) + B_e u(k) + B_d h(k) \\ y(k) = C_p x(k) \end{cases} \tag{3}$$

where

$$Ae = \begin{bmatrix} A_p & B_p \\ \mathbf{0} & 0 \end{bmatrix}_{(n+1)\times(n+1)} \tag{4}$$

$$Be = \begin{bmatrix} B_p & 0 \end{bmatrix}^{\mathrm{T}}_{(n+1)\times 1} \tag{5}$$

$$Ce = \begin{bmatrix} C_p & 0 \end{bmatrix}^{1\times(n+1)} \tag{6}$$

$$Bd = \begin{bmatrix} \mathbf{0} & 1 \end{bmatrix}^{\mathrm{T}}_{(n+1)\times 1} \tag{7}$$

and $x(k) = [x_1(k), x_2(k), ..., x_{n+1}(k)]^{\mathrm{T}}$, $x_{n+1}(k) = d(k)$, $h(k) = d(k) - d(k-1)$. To estimate the disturbances and states of the system, the MESO that is incorporated with model information for NMP system is given as

$$\begin{cases} \hat{x}(k+1) = A_e \hat{x}(k) + B_e u(k) + L_o(\hat{y}(k) - y(k)) \\ \hat{y}(k) = C_e \hat{x}(k) \end{cases} \tag{8}$$

where $\hat{x}(k)$ is the estimated state vector of system Eq.3, and $L_o = [l_1, l_2, ..., l_{n+1}]^{\mathrm{T}}$ is the observer gain.

Through compensating the estimated disturbances for the control action,

$$u(k) = u_0(k) - \hat{x}_{n+1}(k) \tag{9}$$

where $u_0(k)$ is the control action of RC calculated in the following section. The actual system can be behaved as

$$y(k) = P_n(z)(u_0(k) - \hat{x}_{n+1}(k) + d(k)) \approx P_n u_0(k) \tag{10}$$

It is clear that the disturbances can be eliminated from the disturbed system to make the system acts as the identified plant with selecting proper observer gain.

To tune the observer gain, the desired characteristic equation in Eq.8 is given as

$$\Theta(z) = |z\boldsymbol{I} - (A_e - L_o Ce)| = (z - \beta_o)^{n+1} \tag{11}$$

Via implementing the Ackerman formula [22], the observer gain is obtained as

$$L_o = \Theta(Ae) \begin{bmatrix} C_e^{\mathrm{T}} \\ C_e^{\mathrm{T}} A_e^{\mathrm{T}} \\ \cdot \\ \cdot \\ \cdot \\ C_e^{\mathrm{T}} (A_e^{\mathrm{T}})^n \end{bmatrix}^{-1} \begin{bmatrix} 0 \\ 0 \\ \cdot \\ \cdot \\ \cdot \\ 1 \end{bmatrix} \tag{12}$$

It should be noted that a trade-off between the anticipated performance of MESO and its robustness against plant uncertainties or disturbances can be adjusted by designing β_o.

Fig. 3: The basic block of RC to generate periodic signal.

3.2 MESO based Repetitive Control

RC is an effect control algorithm to facilitate performance with repetitive reference or disturbance based on internal model principle. For a discrete conventional RC, a signal generator $z^N/(1\text{-}z^{-N})$, where N is the number of points per period of the reference or disturbance, should be contained in the feedback loop. However, the method magnifies the undesired gain at other frequencies. For precision motion, the non-periodic disturbance can be obvious so that the tracking performance is deteriorated significantly. In this paper, the MESO based Repetitive Control (MESORC) is proposed to compensate undesired disturbances.

To generate a discrete-time periodic signal of length N, the basis block of RC is demonstrated in Fig.3, which can be expressed by the state-space model as

$$\begin{cases} x_{rc}(k+1) = A_{rc} x_{rc}(k) + B_{rc} v(k) \\ w(k) = C_{rc} x_{rc}(k) \end{cases} \tag{13}$$

where

$$A_{rc} = \begin{bmatrix} 0 & 1 & \cdots & 0 \\ \vdots & \vdots & \ddots & \vdots \\ 0 & 0 & \cdots & 1 \\ 1 & 0 & \cdots & 0 \end{bmatrix}_{N\times N} \tag{14}$$

$$B_{rc} = \begin{bmatrix} \mathbf{0} & 1 \end{bmatrix}^{\mathrm{T}}_{N\times 1} \tag{15}$$

$$C_{rc} = \begin{bmatrix} 1 & \mathbf{0} \end{bmatrix}_{1\times N} \tag{16}$$

$v(k)$ and $w(k)$ are the input and output of the block respectively.

Being different the method designed in frequency domain [18, 19], a time-domain method based on state feedback [23] is used in this paper, which has the advantages that no inversion of the modal so that the calculation is simplified.

The proposed control scheme is given in Fig.4. Therefore, the control input of RC is expressed as

$$u_0 = K_{rc} x_{rc}(k) + K_{fb} \hat{x}(k) \tag{17}$$

where $x_{rc}(k)$ and $\hat{x}_p(k)$ are the state vector of Eq.13 and the plant respectively. K_{rc} and K_{fb} are the state feedback matrices for the internal model and the plant, respectively, which is to be determined following. Based on that, Fig.4 has the following equivalent realization,

$$\begin{bmatrix} x_{rc}(k+1) \\ \hat{x}_p(k+1) \end{bmatrix} = \begin{bmatrix} A_{rc} & -B_{rc} C_p \\ 0 & A_p \end{bmatrix} \begin{bmatrix} x_{rc}(k) \\ \hat{x}_p(k) \end{bmatrix} + \begin{bmatrix} 0 \\ B_p \end{bmatrix} + \begin{bmatrix} K_{rc} & K_{fb} \end{bmatrix} \begin{bmatrix} x_{rc}(k) \\ \hat{x}_p(k) \end{bmatrix} \tag{18}$$

To obtain the feedback gains, a linear quadratic regulator (LQR) method is selected to regulate the states and thereby

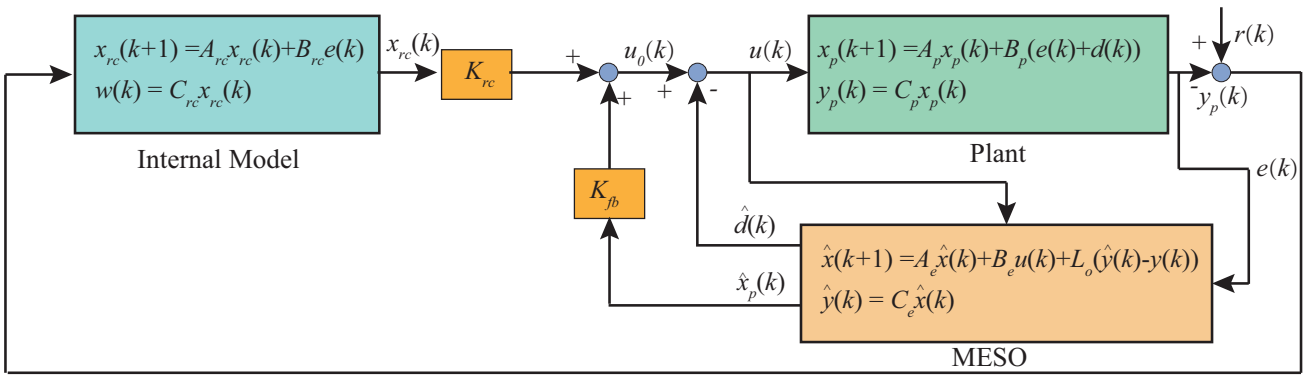

Fig. 4: Block diagram of the proposed control scheme of MESORC.

drive the error to zero. The cost function is given by

$$J=\sum_{k=0}^{\infty}\left\{\sigma(k)^{\mathrm{T}}\begin{bmatrix}Q_1 & 0\\ 0 & Q_2\end{bmatrix}\sigma(k)+u_0(k)^{\mathrm{T}}Ru_0(k)\right\} \tag{19}$$

where Q_1 and Q_2 are symmetric positive definite weighting matrices on the states with $\sigma(k)=[x_{rc}(k),\hat{x}_p(k)]^{\mathrm{T}}$ and R is a symmetric positive definite weighting matrix on the control effort. Therefore, the Eq.18 can be rewritten as

$$\begin{cases}\sigma(k+1)=\begin{bmatrix}A_{rc} & -B_{rc}C_p\\ 0 & A_p\end{bmatrix}\sigma(k)+\begin{bmatrix}0\\ B_p\end{bmatrix}u_0(k)\\ u_0(k)=\begin{bmatrix}K_{rc} & K_{fb}\end{bmatrix}\sigma(k)\end{cases} \tag{20}$$

The above equations can be solved in MATLAB via function *dlqr*. Overall, the control force of the proposed method is calculated as

$$u(k)=K_{rc}x_{rc}(k)+K_{fb}\hat{x}(k)-\hat{x}_{n+1}(k) \tag{21}$$

The main difference of the proposed method and the approach in [23] lies in that a MESO is combined in the control scheme to estimate as well as compensate disturbances and the estimated state variables are also used to designed state feedback based RC for a NMP system under undesired disturbances.

4 Comparative Experiments

In this section, controller implementation and comparative experiments are demonstrated to verify the performance of the proposed method. For the implementation of MESORC, $Q_1=1200000$,$Q_2=1$, $R=0.001$ are selected and the observer gain β_o is determined as 0.696, which results in

$$L_o=[-3352.2-1442.1-1456.7-610.45.488]^{\mathrm{T}} \tag{22}$$

Furthermore, three controllers, proportional plus derivative controller (PI), RC, and MESORC, have been developed for comparisons.

4.1 Suppression of Hysteresis

In this paper, the hysteresis nonlinearity is treated as a low frequency external disturbance without building hysteresis modeling for simple implementation. Experimental results of hysteresis curves with different controllers are displayed in Fig.5 when 1 Hz triangular wave with 10 μm peak-to-peak amplitude is injected into x axis. For the open-loop tracking, the relative maximal error (e_{rmax}) is 20.130%, which exhibit obvious hysteresis nonlinearity. The traditional PI controller can suppress hysteresis partly with e_{rmax} of 1.883%. The RC and MESORC have the similar performance with 0.173% and 0.133%, respectively because the hysteresis nonlinearity behaves periodic errors for periodic triangular waves, which can be compensated by both. The above results demonstrate that the hysteresis is mitigated substantially via implementation the proposed method.

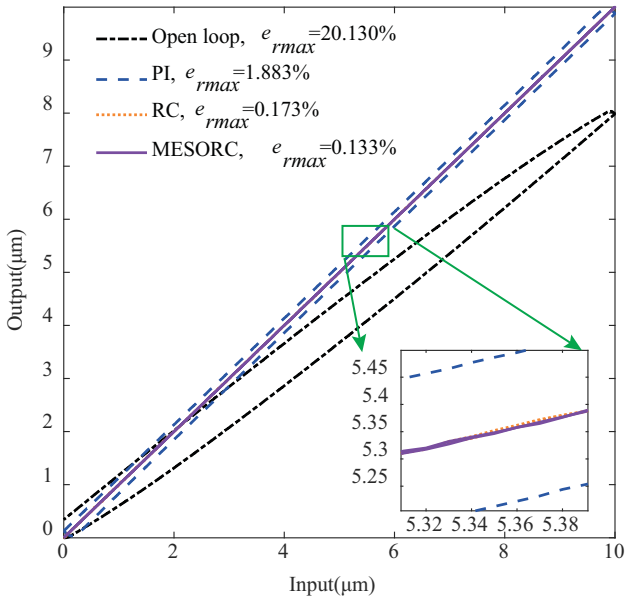

Fig. 5: Experimental results of hysteresis suppression with different controllers.

4.2 High Precision Tracking with Disturbances

In order to validate the tracking performance of the proposed method, the triangular waves widely used in AFMs as references of the fast motion axis for raster scanning are performed on the piezoelectric nanopositioning stage.

4.2.1 Delta Disturbance

The tracking performance of the proposed controller is tested with triangular waves with a maximum 10 μm peak-

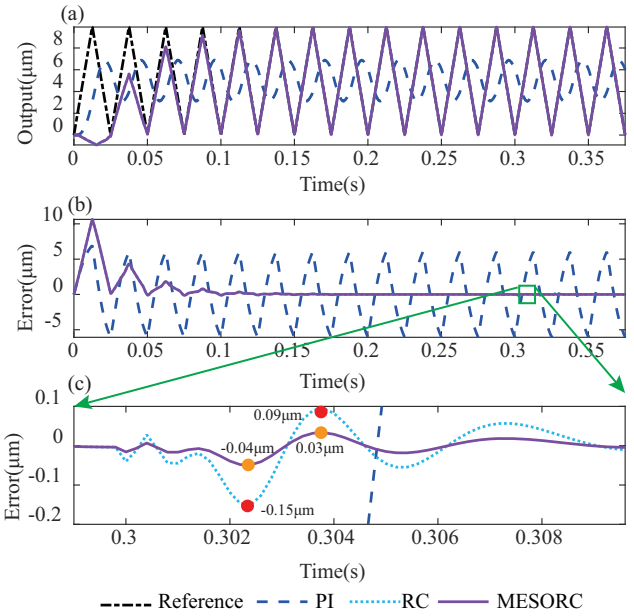

Fig. 6: Experimental results of 40 Hz triangular wave tracking with delta disturbance at 0.3s. (a) Tracking results. (b)Tracking error. (c) Zoomed-in view of the tracking error.

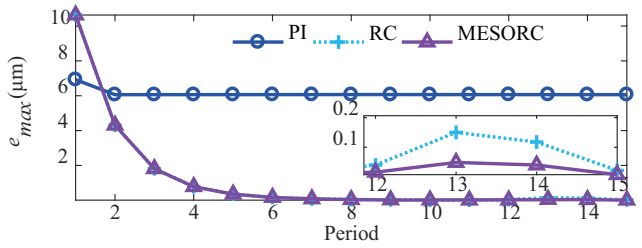

Fig. 7: Experimental results of e_{max} versus period with delta disturbance at 0.3s.

to-peak amplitude at 40 Hz. A delta disturbance is injected into the system at 0.3s. Fig.6 shows the tracking performance with three different controller. It is clear that PI controller exhibit the worst performance for its lowest bandwidth to tracking triangular signals with high-order harmonics with root-mean-square errors (e_{rms}) and maximal errors (e_{max}) of 3.775 μm and 6.069 μm respectively. For both RC and MESORC, the errors are convergent after 0.13s and the e_{rms} and e_{max} are 0.006 μm and 0.014 μm respectively. Experimental results of e_{max} versus period is given in Fig.7. After injecting the delta disturbance, the error peaks of RC are -0.15μm and 0.09 μm, while those of ESORC are -0.04 μm and 0.03 μm, which reduce 73.33% and 66.67%, respectively. It is also clear that at the 13^{th} period, the e_{max} are 0.150 μm and 0.048 μm respectively, which verified the proposed method can compensate delta disturbance effectively.

4.2.2 Chirp Disturbance

The effectiveness of the proposed method to suppress non-periodic disturbance is tested by input an amplitude 0.5 μm chirp signal with frequencies varying from 0.01 Hz to 20 Hz that is defined as a time-varying signal on the 40 Hz triangular reference. The tracking results as well as steady-state tracking errors are given in Fig. 8 and the statistical

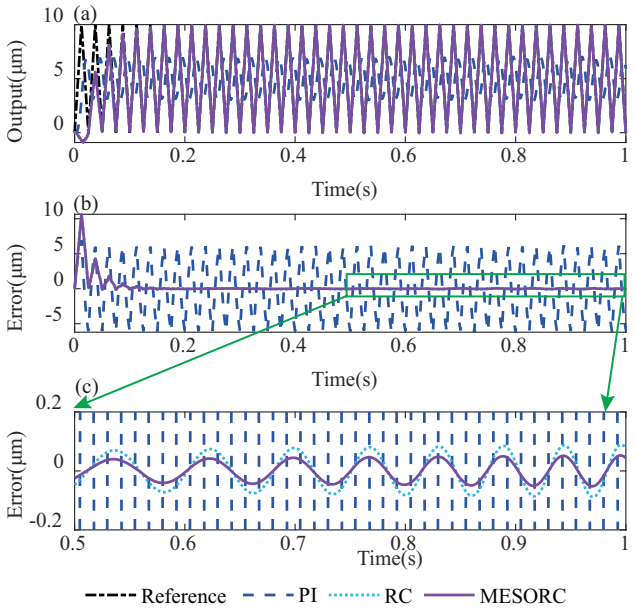

Fig. 8: Experimental results of 40 Hz triangular wave tracking with chirp disturbance. (a) Tracking results. (b)Tracking error. (c) Zoomed-in view of the steady-state tracking error.

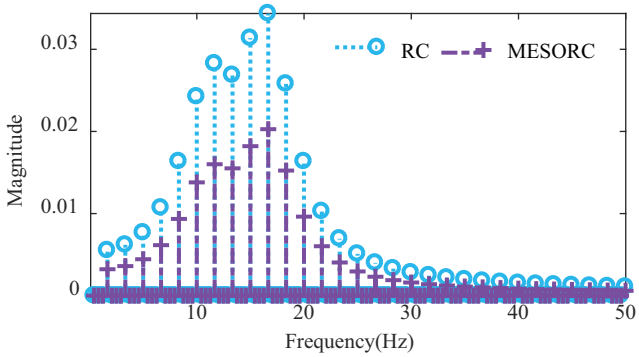

Fig. 9: Spectrum of steady-state errors with chirp disturbance.

results of steady-state errors are listed in Tab. 1. Similar to previous results, PI controller's performance is the worst with e_{rms} of 3.759 μm and e_{max} of 6.179 μm respectively. Compared with RC , MESORC can cope with non-periodic disturbances effectively, as is showed in Fig. 8. The e_{rms} and e_{max} with the proposed controller reduce 40.98% (from 0.061 μm to 0.036 μm) and 41.57% (from 0.089 μm to 0.052 μm) respectively with respect to the condition with RC. The spectrum of steady-state errors with chirp disturbances is demonstrated in Fig. 9. It is evident that MESORC can compensated errors at those frequencies effectively in comparison with standalone RC. The estimated disturbance of MESORC is also plotted in Fig. 10, which verifies the chirp disturbance is estimated accurately so that MESORC can achieve better performance. Overall, errors caused by both periodic and non-periodic disturbance can be suppressed significantly with the proposed method.

5 Conclusions

In this paper, a composite control scheme MESORC is proposed to achieve high precision motion for piezoelectric nanopositioning stages with periodic reference even un-

Table 1: Statistical results of steady-state errors with different controller under chirp disturbance

Controller	e_{rms}	e_{max}
PI	3.759 μm	6.179 μm
RC	0.061 μm	0.089 μm
MESORC	0.036 μm	0.052 μm

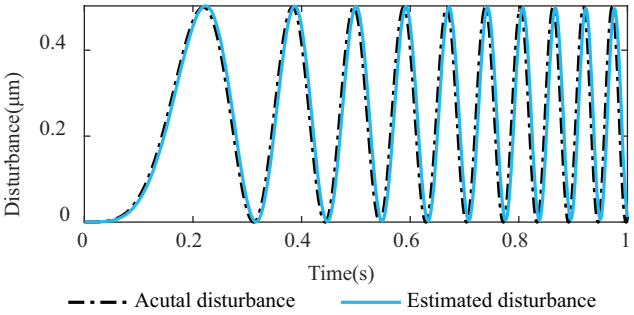

Fig. 10: Experimental results of compensation on chirp disturbance. (a) Actual disturbance . (b) Estimated disturbance

der unexpected disturbance. The hysteresis nonlinearity is treated as low-frequency disturbance to avoid hysteresis modeling and simplify controller implementation and the proposed method is developed in time domain. The MESO is utilized to handle with the NMP property of the system and estimated the state variables and disturbances simultaneously. Based on the estimated results, a state feedback based RC is develop to compensate periodic errors. To validate the performance, the proposed method is also performed on a piezoelectric nanopositioning stage. Experimental results show that the proposed method can suppress low frequency hysteresis effectively and achieve the best performance with the triangular waves references up to 40 Hz with delta and chirp disturbances of on the stage through comparing with various controllers.

References

[1] M. Rana, , H. Pota, and I. Petersen. Improvement in the Imaging Performance of Atomic Force Microscopy: A Survey, *IEEE Transactions on Automation Science and Engineering*, 14(2): 1265-1285, 2017.

[2] W. Y. Liang, J. Ma and K. K. Tan. Contact Force Control on Soft Membrane for an Ear Surgical Device, *IEEE Transactions on Industrial Electronics*, 65(12): 9593-9603, 2018.

[3] Y. Tian, D. Zhang, and B. Shirinzadeh, Dynamic modelling of a flexure-based mechanism for ultra-precision grinding operation, *Precision Engineering*, 35(4) : 554565, 2011.

[4] Y. Yong , S. Moheimani, B. Kenton, K. Leang, Invited review article: High-speed flexure-guided nanopositioning: Mechanical design and control issues, *Review of scientific instruments*, 83(12): 121101, 2012.

[5] G. Y. Gu, L. M. Zhu, , C. Y. Su, H. Ding, S Fatikow, Modeling and Control of Piezo-Actuated Nanopositioning Stages: A Survey, *IEEE Trans. Automation Science and Engineering*, 13(1): 313-332, 2016 .

[6] Z. Guo, Y Tian, X. Liu, B. Shirinzadeh, F. Wang, D. Zhang, An inverse PrandtlIshlinskii model based decoupling control methodology for a 3-DOF flexure-based mechanism, *Sensors and Actuators A: Physical*, 230: 52-62, 2015.

[7] D. Habineza, M. Rakotondrabe, Y. Le Gorrec, BoucWen modeling and feedforward control of multivariable hysteresis in piezoelectric systems: application to a 3-dof piezotube scanner, *IEEE Transactions on Control Systems Technology*, 23(5): 1797-1806, 2015.

[8] J. Shan, Y. Liu, U. Gabbert, N. Cui, Control system design for nano-positioning using piezoelectric actuators, *Smart Materials and Structures*, 25(2): 025024, 2016.

[9] J. Y. Lau, W. Y. Liang, H. C. Liaw, K. K. Tan, Sliding mode disturbance observerbased motion control for a piezoelectric actuatorbased surgical device, *Asian Journal of Control*, 20(3): 1194-1203, 2018.

[10] J. Y. Lau, W. Y. Liang, K. K. Tan, Enhanced robust impedance control of a constrained piezoelectric actuator-based surgical device, *Sensors and Actuators A: Physical*, 290: 97-106, 2019.

[11] Z. Feng, J. Ling, M. Ming, X. H. Xiao, High-bandwidth and flexible tracking control for precision motion with application to a piezo nanopositioner, *Review of Scientific Instruments*, 88(8): 085107, 2017.

[12] J. Yi, S. Chang, Y. Shen, Disturbance-observer-based hysteresis compensation for piezoelectric actuators, *IEEE/ASME Transactions on Mechatronics*, 14(4): 456-464, 2009.

[13] I. R. Petersen, Negative imaginary systems theory and applications, *Annual Reviews in Control*, 42: 309-318, 2016.

[14] H. Habibullah, H. R. Pota, I. R. Petersen, A novel control approach for high-precision positioning of a piezoelectric tube scanner, *IEEE Transactions on Automation Science and Engineering*, 14(1): 325-336, 2017.

[15] B. A. Francis, W. M. Wonham, The internal model principle of control theory, *Automatica*, 12(5): 457-465, 1976.

[16] Y. Wang, F. Gao, F. J. Doyle III, Survey on iterative learning control, repetitive control, and run-to-run control, *Journal of Process Control*, 19(10): 1589-1600, 2009.

[17] Y. Shan, K. K. Leang, Dual-stage repetitive control with PrandtlIshlinskii hysteresis inversion for piezo-based nanopositioning, *Mechatronics*, 22(3): 271-281, 2012.

[18] C. X. Li, G. Y. Gu, M. J. Yang, L. M. Zhu, High-speed tracking of a nanopositioning stage using modified repetitive control, *IEEE Transactions on Automation Science and Engineering*, 14(3): 1467-1477, 2017.

[19] C. X. Li, G. Y. Gu, L. M. Zhu, C. Y. Su, Odd-harmonic repetitive control for high-speed raster scanning of piezo-actuated nanopositioning stages with hysteresis nonlinearity. *Sensors and Actuators A: Physical*, 244: 95-105, 2016.

[20] W. H. Chen, J. Yang, L. Guo, S. Li, Disturbance-observer-based control and related methodsAn overview, *IEEE Transactions on Industrial Electronics*, 63(2): 1083-1095, 2016.

[21] L. Sun, D. Li, Z. Gao, Z. Yang, S. Zhao, Combined feedforward and model-assisted active disturbance rejection control for non-minimum phase system, *ISA transactions*, 64: 24-33, 2016.

[22] C. Fu, W. Tan, Tuning of linear ADRC with known plant information, *ISA transactions*, 65: 384-393,2016.

[23] C. T. Freeman, M. A. Alsubaie, Z. Cai, E. Rogers, P. L. Lewin, A common setting for the design of iterative learning and repetitive controllers with experimental verification, *International Journal of Adaptive Control and Signal Processing*, 27(3): 230-249, 2013.